Zeolites | Hot Paper

HPM-16, a Stable Interrupted Zeolite with a Multidimensional Mixed Medium–Large Pore System Containing Supercages

Zihao Rei Gao, Salvador R. G. Balestra, Jian Li,* and Miguel A. Camblor*

Abstract: *HPM-16 is a highly porous germanosilicate zeolite with an interrupted framework that contains a three-dimensional system of $12 + 10 \times 10(12) \times 12 + 10$-membered ring (MR) pores. The 10(12) MR pore in the b direction is a 10 MR pore with long 12 MR stretches forming 30 Å long tubular supercages. Along one direction the 10 MR pores are fused, meaning that the separation between adjacent pores consists of a single tetrahedron that is, additionally, connected to only three additional tetrahedra (a Q^3). These fused pores are thus decorated by T-OH groups along the whole diffusion path, creating a hydrophilic region embedded in an otherwise essentially hydrophobic environment. The structure is built from highly porous $12 \times 12 \times 12$ MR uninterrupted layers that are connected to each other through Q^3 producing a second system of $10 \times 10 \times 10$ MR pores. This zeolite can be extensively degermanated yielding a material with high thermal stability, despite its interrupted nature.*

Zeolites are classically defined as crystalline microporous tectosilicates.[1] This implies that their ordered structures are built by silicon (aluminum) oxide tetrahedra that share all their oxygen atoms once and only once with neighboring tetrahedra. The Structure Commission of the International Zeolite Association (IZA) assigns a three-letter code to each accepted zeolite topology.[2] However, zeolite-like topologies in which not all the tetrahedra are 4-connected, the so-called zeolite interrupted frameworks,[3] are also assigned IZA codes preceded by a hyphen and are also collected in the database of Zeolite Structures.[2] The wide applicability of zeolites relies on their large diversity of structures, chemical compo-

sitions and physicochemical properties. For instance, pure silica zeolites with no Si–OH groups are strictly hydrophobic, while the presence of -OH groups increases their hydrophilicity.[4] The hydrophilic/hydrophobic character of zeolites may largely influence their performance in catalysis and adsorption processes.[5] On the other hand, zeolites with a mixed 12×10 MR channel system were once highly sought after because they could provide special shape selectivity properties,[6] which was later confirmed.[7] Large cavities in zeolites, often called supercages, are also attractive as confined spaces for the ship-in-a-bottle inclusion of species active in catalytic or sensing applications.[8] Here we present an interrupted germanosilicate zeolite framework with a new highly porous topology containing a mixed 10/12 MR 3D pore system and mixed hydrophilic/hydrophobic environments. This is the only zeolite topology that contains a 2D system of interconnected 12 MR pores plus a 3D system of interconnected 10 MR pores. Straight 10 and 12 MR pores run along [100] and [001], while in the [010] direction the two systems are interconnected through large (30 Å long) elongated supercages constituting an undulated 10 MR pore. After degermanation, this zeolite displays an outstanding thermal stability.

HPM-16 was synthesized as a germanosilicate using 1-methyl-2-ethyl-3-*n*-propylimidazolium (1M2E3nPrIM) and fluoride as structure-directing agents (Section S1 in Supporting Information, SI). The Ge fraction, $Ge_f = Ge/(Si + Ge)$, in the crystals was determined by Energy-Dispersive X-ray Spectroscopy (EDS) to be 0.30, which is coincident with the Ge_f value in the synthesis gel (Table S1). Typically, HPM-16 is composed of individual and twinned tablet-shaped crystals with an approximate crystal size around $2 \times 1 \times 0.1$ μm³ (Figure S1b), while some samples synthesized in different conditions consisted of larger crystallites in the form of highly twinned gear-like crystals (Figure S1a). The structure of HPM-16 was solved using 3D electron diffraction (3D ED) and Rietveld refined against synchrotron powder X-ray diffraction (PXRD) data (Figure 1), and details can be found in SI (Section S2.1–S2.2, Table S2–S8, and Figure S2–S4).

The micropore system of HPM-16 can be described as a 3D $12 + 10 \times 10(12) \times 12 + 10$ MR intersecting pore system. The 12 MR pores are 2D, straight, intersect each other and run along [001] and [100] (Figure 2A,B) with a crystallographic size of 7.8×6.8 Å and 9.0×5.7 Å (Figure S5), respectively. Along [010] (Figure 2C) the 10(12) description refers to the existence of long stretches of 12 MR pores that are connected only through 10 MR (size 5.7×4.9 Å and 6.0×5.2 Å, Figure S5), yielding an elongated $[4^{10}6^8 10^8 12^4]$ supercage 30 Å long, with access through 10 and 12 MR windows

[*] Z. R. Gao, Dr. S. R. G. Balestra, Prof. Dr. M. A. Camblor
Instituto de Ciencia de Materiales de Madrid
Consejo Superior de Investigaciones Científicas (ICMM-CSIC)
c/ Sor Juana Inés de la Cruz, 3, 28049 Madrid (Spain)
E-mail: macamblor@icmm.csic.es

Dr. J. Li
Berzelii Center EXSELENT on Porous Materials
Department of Materials and Environmental Chemistry
Stockholm University
10691 Stockholm (Sweden)
E-mail: jxpxlijian@pku.edu.cn

Supporting information and the ORCID identification number(s) for the author(s) of this article can be found under:
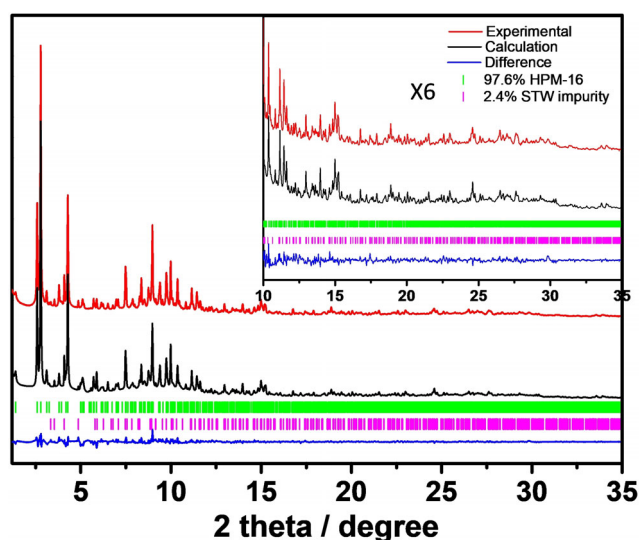https://doi.org/10.1002/anie.202106734.

Figure 1. Rietveld refinement plot ($\lambda = 0.618668$ Å) for as-made HPM-16 (containing a small, <3%, STW impurity, see SI). Red: experimental, black: calculated, blue: difference. Vertical bars are allowed reflections for HPM-16 (green) and STW (purple). CCDC NO. 2097880 and 2097878 for as-made and calcined HPM-16, respectively.

Figure 3. The supercages in HPM-16 and MWW: a) the disordered OSDAs in the supercage of HPM-16, showing the OSDA locations at two distinct 10 MR and 12 MR channel intersections, b) 30.0 Å length $[4^{10}6^{8}10^{8}12^{4}]$ supercage in HPM-16 and c) 18.8 Å length $[5^{12}6^{14}10^{6}]$ supercage in MWW.

(Figure 3b). The 10 MR pores also constitute a 3D system of straight pores that intersect each other and run along [001] and [100] plus an undulating pore running along [010]. The supercage, in which OSDA cations are found disordered (Figure 3a), is much larger than the elongated $[5^{12}6^{14}10^{6}]$ supercage found in MWW (18.8 Å, Figure 3c), open through 10 MR windows.[9] The straight 10 MR pores in HPM-16 are rather peculiar: two rows of fused 10 MR channels exist along
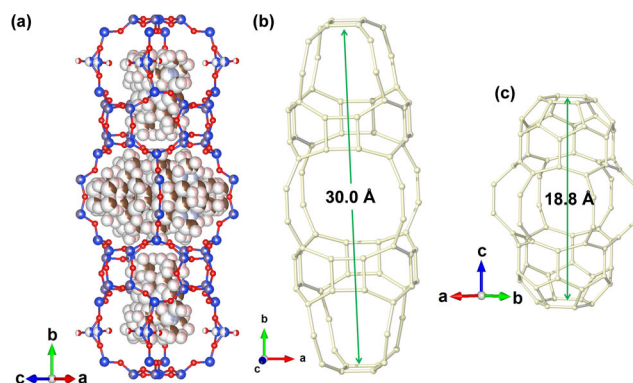
the *c*-axis due to the presence of Q^3 atoms close to $y = 0.25$ and 0.75 along this direction (Figure 2 A); the Q^3 atoms show disorder; along the *a*-axis, the 10 MR are separated by two bonded Q^3 atoms (Figure 2 B). The pore system of HPM-16 was characterized using the PoreBlazer 4.0, RASPA, and iRASPA codes[10] (Figure S6 and Section S3.4), resulting in reasonable agreement with the experimental porosity of a freshly calcined zeolite tested by Ar adsorption/desorption (Figure S7), which allowed to determine a pore size distribution with maxima at 6.7, 7.9, and 9.0 Å (Figure S8). From N_2 adsorption/desorption experiments (Figure S9) a BET surface area of 535 $m^2 g^{-1}$ and a *t*-plot micropore volume of 0.20 $cm^3 g^{-1}$ were determined.
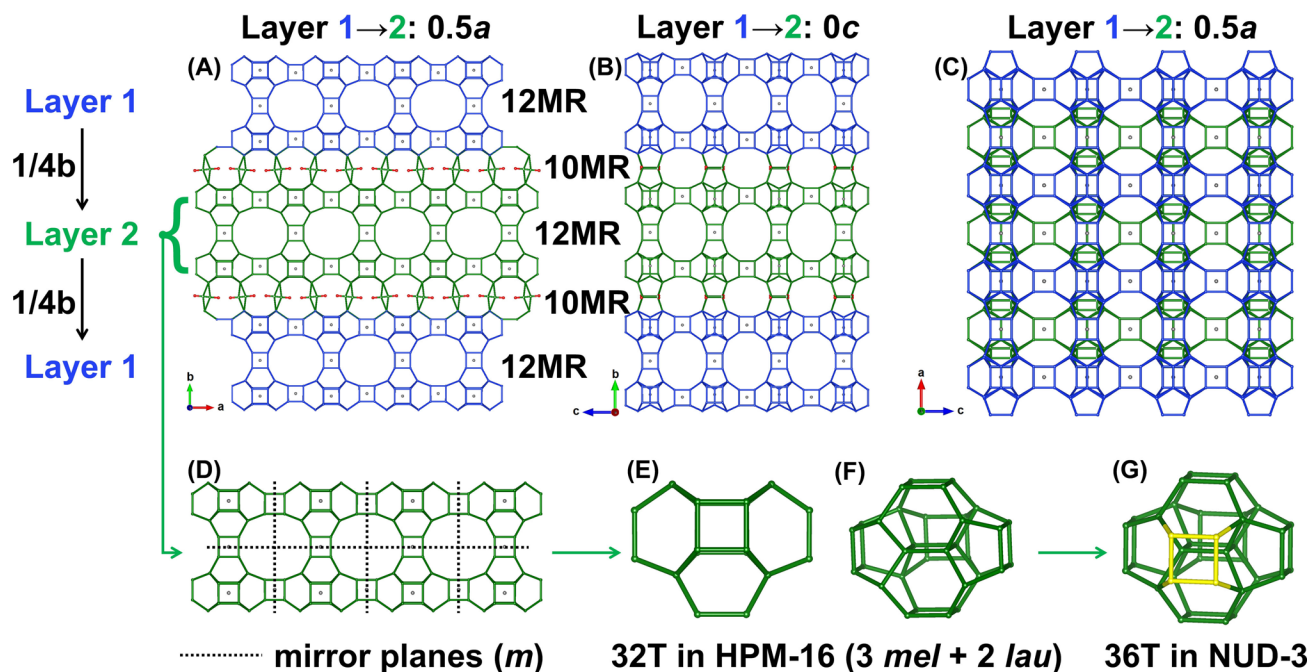

Figure 2. Structure of HPM-16: along A) [001], B) [100], and C) [010]; D) the 23 Å thick HPM-16-layer, E,F) the 32 T half-open unit (3 *mel* + 2 *lau*) in HPM-16, G) the 36 T closed unit (4 *mel* + 2 *lau*) in NUD-3. Only T–T connections and T-OH (red) are shown. A–C) T atoms in green and blue correspond to the layer with or without a lateral shift (0.5*a*, 0.25*b*, 0*c*), respectively, F,G) T atoms in yellow show the difference of the units in HPM-16 and NUD-3. Small unconnected balls in (A–D) show the fluoride sites in the as-made material.

The framework of this new zeolite can be built using 23 Å thick, highly porous (3D 12 MR), mirror-symmetric layers (Figure 2D) connected to each other along *b* through Q^3 TO_4 tetrahedra, thus bearing some resemblance to the so-called Interlayered Expanded Zeolites (IEZ) in which a post-synthetic reaction of a layered material with an appropriate silane introduces a Q^2 site that joins the layers.[11] Within the HPM-16 layer, there is a half-open unit built by 32 T-atoms (Figure 2E), constructed of 3 *mel*, i.e. $[4^5 6^4]$, and 2 *lau*, i.e. $[4^2 6^4]$ units (Figure 2F), that is similar to the 36-T-atom closed unit in the recently reported NUD-3 (Figure 2G), which is composed of 4 *mel* and 2 *lau* units.[12] The 32 T-atom half-open unit in HPM-16 could be regarded as the 36 T-atoms unit in NUD-3 lacking one of the single 4 rings (s4r). The half-open units are connected through d4r along the [100] and [001] directions, forming a 2D infinite layer. Then, the neighboring layers are connected after a lateral shift of 0.5*a* along the [010] direction via Q^3 TO_4 tetrahedra, thus forming an interrupted 3D zeolite framework. Rietveld refinement shows that all these Q^3 T atoms are disordered, which is simulated by these atoms having two orientations at $y = 0.25$ and 0.75. As a result of the large thickness of the layers involved, the value of the *b*-axis in HPM-16 is very long.

The ^{29}Si magic-angle-spinning (MAS) NMR spectrum (Figure S10a) shows three resonances at −96.6, −103.7, and −121.6 ppm. The resonance at −96.6 ppm could be assigned to Q^2 Si atoms, that is, $\underline{Si}(OSi)_2(OH)_2$, or Q^3 Si atoms with a neighboring Ge atom, that is, $\underline{Si}(OSi)_2(OGe)(OH)$. Considering the structure model from cRED structure solution and Rietveld refinement, the resonance at −96.6 ppm is assigned to $\underline{Si}(OSi)_2(OGe)(OH)$ Q^3 Si atoms. The resonances at −103.7 and −121.6 ppm are assigned to Q^4 sites with acute and obtuse, respectively, average T-O-T angles.[13] These ^{29}Si MAS NMR spectra proved that the framework of HPM-16 contains both Q^3 and Q^4 Si and deconvolution of the spectrum showed that the Q^3/Q^4 Si ratio is around 5.0%, which matched well with the structure solution (5.9%). The ^{19}F solid state NMR spectrum of HPM-16 presents two resonances at −20.6 and −9.4 ppm (Figure S11), assigned to F⁻ anions in d4r units of type II and III, respectively, that is, d4r with isolated Ge or with Ge pairs not involved in larger clusters (with no Ge having three Ge neighbors), respectively.[14] The Rietveld refinement results show in fact that the d4r are enriched in Ge ($Ge_f = 0.40–0.54$), while the other sites are Ge-poor ($Ge_f = 0–0.18$; see cif files in SI). The ^{13}C solid state NMR spectrum of an as-made HPM-16 sample (Figure S12a) matched well with the ^{13}C liquid NMR spectrum of the bromide form of the OSDA in D_2O (1M2E3nPrIM⁺ bromide, Figure S12b). This indicates that the OSDA is essentially intact in the as-made zeolite, which is also proved by the C,H,N elemental analysis (Table S1) giving a C/N ratio of 4.55, very close to the value in the OSDA (4.5). The experimental value of the H/N ratio (10.31) is significantly higher than the calculated one (8.5), which could be explained by the existence of some water (in agreement with a low-temperature weight loss step in the TG, Figure S13) and the aforementioned T-OH groups. The existence in as-made HPM-16 of both water and T-OH groups is also strongly supported by infrared spectra of a self-supported wafer before and after dehydration (Figure S14).

HPM-16 is stable upon calcination at 550°C but its crystallinity decreases after exposure to ambient air at room temperature (Figure S15). After removal of the OSDA by ozone treatment, HPM-16 was subjected to several runs of degermanation in an alcoholic acidic solution (Section S1.5), and the results were followed by EDS and PXRD. The Ge_f values within the crystals, together with the unit cell parameters and volumes, decrease gradually (Table S9) and show a good linear relationship. The calculation of the averaged cell volume of the zeolite with $Ge_f = 0$ yields a cell volume that is in good agreement with the value predicted by the linear fitting of the experimental results (Figure S16). Finally, the Ge_f in degermanated HPM-16 dropped to 0.09 and this material showed a very good thermal stability upon calcination at 800°C (Figure 4), although treatment at 200°C in water for 24 hours produced a limited decrease in crystallinity. The ^{29}Si MAS NMR spectrum of the degermanated sample (Figure S10b) shows resonances at −119.5 and −110 ppm. Under cross polarization (CP) conditions (Figure S10c) the intensity of a Q^3 resonance at −101.4 ppm is largely increased relative to the ones at −110 or −119.5 ppm. The latter are both attributed to Q^4 in different crystallographic sites with acute or obtuse Si-O-Si angles, respectively.[13] According to the Rietveld refinement of the degermanated sample (Figure S17 and Table S10–S12; CCDC NO. 2097879) sites Si7 and Si9, with average angles of 165.3° and 162.7°, respectively, may be responsible for the high-field signal (predicted chemical shifts −121.2 and −119.7 ppm, respectively). All other T sites have more acute angles (144–152°). Degermanated HPM-16 has strong OH vibrations after dehydration (Figure S18).

The existence in HPM-16 of pairs of Q^3 sites at fractional *y* values close to 0.25 and 0.75 that are not very far apart (around 5.9 Å) raised the question of whether it could be possible to condense them by direct synthesis in other conditions or by post-synthetic treatments of HPM-16. Such condensation of Q^3 pairs that would yield s4r can be discarded
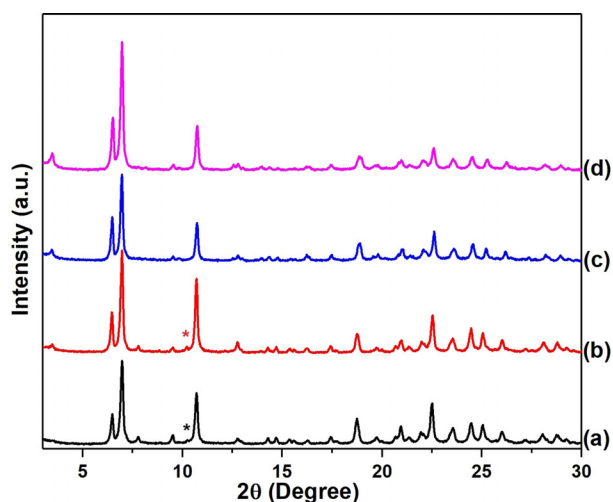

Figure 4. Powder X-ray diffraction patterns of HPM-16: a) as-made, b) after ozone treatment, c) after final run of degermanation, and d) calcined at 800°C after final run of degermanation. * marks a trace impurity of STW in the as-made and ozone treated samples (a,b). This disappears during the degermanation treatment (c,d).

in the actual HPM-16 mainly based on Rietveld refinement results, although the existence of disorder (represented by two T positions with partial occupancies) might introduce some uncertainty. To study the issue, we generated a set of ten derived polymorphs (Figure S19), which for completeness also included the conversion of the generated s4r into d4r, and calculated their formation energies (see SI). As SiO_2 polymorphs, they all were much less stable than typical high silica or pure silica zeolites (over $18\, kJ\, mol^{-1}$ relative to quartz compared to at most $15\, kJ\, mol^{-1}$ reported by Navrotsky et al. and Piccione et al.; Table S13).[15] However, the same calculation for STW gave an energy similar to those of the derived polymorphs, which is interesting: this zeolite has been argued to be possible as a pure SiO_2 zeolite only because of the facilitating polarizing effect of fluoride, which makes the zeolite more flexible and allows its crystallization.[16] That means the polymorphs under consideration may be difficult to realize but still possible. In this respect, we may consider the case of one of the derived polymorphs, which is isostructural to the recently reported NUD-3.[12] This is the polymorph with the lowest energy among those considered, but still too high to be taken as feasible under this kind of considerations. However, NUD-3 has already been prepared, although so far only as a germanosilicate. When the energies of the GeO_2 polymorphs are considered, they are found to be much smaller (lower energies compared to quartz-type GeO_2) and in that case well below the $15\, kJ\, mol^{-1}$ feasibility limit (Table S14). Given that what is actually synthesized is always an organic–inorganic hybrid compound where host–guest interactions may significantly alter the stability (as in the STW case commented above) and since NUD-3 has a real existence, the future preparation of some of the polymorphs considered here cannot be discarded.

In summary, the new HPM-16 zeolite has been synthesized as a germanosilicate using 1-methyl-2-ethyl-3-*n*-propylimidazolium and fluoride and its structure has been solved using electron diffraction and refined against synchrotron diffraction data. It presents a new interrupted topology containing a 2D system of large 12 MR pores and a 3D system of medium 10 MR pores. HPM-16 may be extensively degermanated, yielding a highly stable zeolite.

[1] M. A. Camblor, S. B. Hong in *Porous Materials*, (Eds.: D. W. Bruce, D. O'Hare, R. I. Walton), Wiley, Chichester, **2011**, pp. 265–325.

[2] C. Baerlocher, L. B. McCusker, *Database of Zeolite Structures*: http://www.iza-structure.org/databases/, accessed on Feb. 26th, **2021**.

[3] L. B. McCusker, F. Liebau, G. Engelhardt, *Pure Appl. Chem.* **2001**, *73*, 381–394.

[4] T. Blasco, M. A. Camblor, A. Corma, P. Esteve, J. M. Guil, A. Martínez, J. A. Perdigón-Melón, S. Valencia, *J. Phys. Chem. B* **1998**, *102*, 75–88.

[5] M. A. Camblor, A. Corma, S. Iborra, S. Miquel, J. Primo, S. Valencia, *J. Catal.* **1997**, *172*, 76–84.

[6] M. E. Davis, R. F. Lobo, *Chem. Mater.* **1992**, *4*, 756–768.

[7] R. Simancas, D. Dari, N. Velamazán, M. T. Navarro, A. Cantín, J. L. Jordá, G. Sastre, A. Corma, F. Rey, *Science* **2010**, *330*, 1219–1222.

[8] a) K. J. Balkus, M. Eissa, R. Levado, *J. Am. Chem. Soc.* **1995**, *117*, 10753–10754; b) P. Payra, P. K. Dutta, *Microporous Mesoporous Mater.* **2003**, *64*, 109–118; c) J. V. Ros-Lis, R. Martínez-Máñez, J. Soto, L. A. Villaescusa, K. Rurack, *J. Mater. Chem.* **2011**, *21*, 5004–5010; d) Y. Yu, J. Mai, L. Wang, X. Li, Z. Jiang, F. Wang, *Sci. Rep.* **2014**, *4*, 5997.

[9] V. V. Narkhede, H. Gies, *Chem. Mater.* **2009**, *21*, 4339–4346.

[10] a) D. Dubbeldam, S. Calero, D. E. Ellis, R. Q. Snurr, *Mol. Simul.* **2016**, *42*, 81–101; b) D. Dubbeldam, S. Calero, T. J. H. Vlugt, *Mol. Simul.* **2018**, *44*, 653–676; c) L. Sarkisov, R. Bueno-Perez, M. Sutharson, D. Fairen-Jimenez, *Chem. Mater.* **2020**, *32*, 9849–9867.

[11] a) S. Inagaki, T. Yokoi, Y. Kubota, T. Tatsumi, *Chem. Commun.* **2007**, *48*, 5188–5190; b) H. Gies, U. Müller, B. Yilmaz, T. Tatsumi, B. Xie, F.-S. Xiao, X. Bao, W. Zhang, D. De Vos, *Chem. Mater.* **2011**, *23*, 2545–2554.

[12] F.-J. Chen, Z. R. Gao, J. Li, L. Gómez-Hortigüela, C. Lin, L. Xu, H.-B. Du, C. Márquez-Álvarez, J. Sun, M. A. Camblor, *Chem. Commun.* **2021**, *57*, 191–194.

[13] J. M. Thomas, J. Klinowski, S. Ramdas, B. K. Hunter, D. T. B. Tennakoon, *Chem. Phys. Lett.* **1983**, *102*, 158–162.

[14] R. T. Rigo, S. R. G. Balestra, S. Hamad, R. Bueno-Perez, A. R. Ruiz-Salvador, S. Calero, M. A. Camblor, *J. Mater. Chem. A* **2018**, *6*, 15110–15122.

[15] a) A. Navrotsky, I. Petrovic, Y. Hu, C.-Y. Chen, M. E. Davis, *Microporous Mater.* **1995**, *4*, 95–98; b) P. M. Piccione, C. Laberty, S. Yang, M. A. Camblor, A. Navrotsky, M. E. Davis, *J. Phys. Chem. B* **2000**, *104*, 10001–10011.

[16] A. Rojas, M. A. Camblor, *Angew. Chem. Int. Ed.* **2012**, *51*, 3854–3856; *Angew. Chem.* **2012**, *124*, 3920–3922.
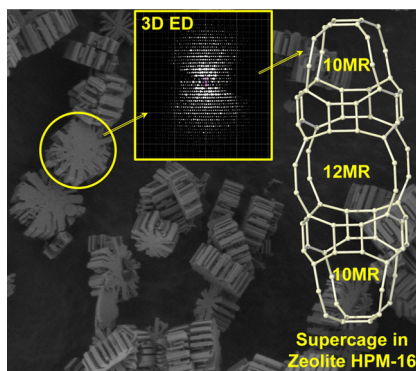
Communications

Zeolites

Z. R. Gao, S. R. G. Balestra, J. Li,*
M. A. Camblor* —————— ▮▮▮▮–▮▮▮▮

HPM-16, a Stable Interrupted Zeolite with
a Multidimensional Mixed Medium–
Large Pore System Containing
Supercages

Supercage in
Zeolite HPM-16

HPM-16 is a new interrupted zeolite with
3D intersecting $12+10\times10(12)\times12+$
10 MR channels containing 30 Å long
supercages. The structure, with a very
long b-axis (>50 Å), was solved by state-
of-the-art 3D electron diffraction. Deger-
manated HPM-16 is stable up to 800°C.
Several derived structures were studied,
including one recently reported.